Study of Helium-based Drift Chamber Gases

K.K. Gan, C.M. Daubenmier, H. Kagan, R. Kass

Department of Physics, The Ohio State University, Columbus, OH 43210, U.S.A.

A.J. Sadoff

Ithaca College, Ithaca, NY 14850, U.S.A.

Abstract

The spatial resolution and dE/dx resolution of several helium-based drift chamber gases have been measured and compared with an argon-based gas, ArC_2H_6 (50:50). The gases were investigated with a system of aluminum drift tubes using cosmic rays. The gases studied include various mixtures of helium and ethane, isobutane, and propane. The spatial resolution of the helium-based gases is better than that of ArC_2H_6 (50:50), while the dE/dx resolution is comparable.

1 Introduction

A high-resolution, low-mass drift chamber is one of the detector requirements to study K meson, charm and bottom quarks, and τ lepton decays at the next generation of e^+e^- experiments. The momenta of most of the particles produced in these experiments are below 1 GeV/c and multiple scattering is a limiting factor in the momentum measurement. Consequently, a gas mixture based on a low-Z molecule is preferred. In addition, a low-mass gas has an advantage over argon-based gases in that it is more transparent to synchrotron radiation. This could be an important feature as these new high luminosity e^+e^- colliders may produce large amounts of synchrotron radiation in the interaction region.

Various mixtures of helium-based gases have been studied by several groups. The first large drift chamber to use a helium-based gas measured a spatial resolution [1] of 260 μm for a mixture with 6% propane (C_3H_8). More recently, there are measurements [2–5] of different mixtures of helium with ethane (C_2H_6), isobutane (C_4H_{10}), dimethylether (DME), and isobutane plus CO_2.

Preprint submitted to Elsevier Science *29 November 1995*

In this paper, we present a study of various mixtures of helium with ethane, propane, and isobutane. The mixtures studied were chosen to have the desired properties for the new CLEO III drift chamber [6], which has a shorter tracking length in comparison with the present CLEO II drift chamber [7]. The new chamber is designed to have momentum resolution and specific energy loss (dE/dx) resolution comparable to the CLEO II chamber. Consequently, the properties of the argon-ethane (50:50) mixture currently used in the CLEO II chamber are also measured for a direct comparison.

2 Test Chamber

A test chamber was constructed specifically for these gas studies. The test chamber consists of three groups of ten aluminum drift tubes as shown in Fig. 1. The sense wires are gold-plated tungsten with a diameter of 20 μm. The tubes are mounted in an aluminum frame. The aluminum tubes have an inner diameter of 2.0 cm and length of 38 cm. The thickness of the tube walls is 0.9 mm. A short section of $\sim$3 cm long near the middle of each tube is ground to a thickness $\sim$0.3 mm to allow the use of Fe^{55} to test the operation of the chamber with ArC_2H_6 (50:50). The inner diameter of these tubes is slightly larger than the cell size of the current design for the CLEO III drift chamber. The cylindrical geometry is chosen to simplify the measurement of the property of the gases. The system is triggered by a coincidence of the top (S2 or S3) and bottom (S1) scintillators. For a track to be used in the spatial and dE/dx resolution measurements, it must also pass through one of the two pairs of narrow counters (S4·S5 or S6·S7). The width of these counters is $\sim$7 cm and the distance between S4/S6 and S5/S7 is $\sim$45 cm. For the spatial resolution measurement, this minimizes the difference in the propagation time for the signal in the top and bottom tubes to reach the electronics. For the dE/dx resolution measurement, this selects vertical tracks so that the path length in a tube can be calculated from the drift distance. For this measurement, the tracks must also pass through $\sim$40 cm of lead/iron and register a hit in S8. This eliminates most of the tracks with momenta less than 400 MeV/c which have a large range of dE/dx loss.

The signal from the wires was amplified using a pre-amplifier with a gain of 5.1 mV/μA. The signal was then split for the drift time and pulse height measurements. For the drift time measurement, the signal was discriminated using LeCroy NIM Discriminator 620 or 623 and then digitized with LeCroy CAMAC TDC2228, set at 0.5 ns/count. The threshold was set at 50 mV to keep drift tube single rates below 100 Hz. The pulse height was digitized using LeCroy CAMAC ADC2249A. The width of the ADC gates is $\sim$500 ns, corresponding to the maximum drift time of one of the helium-based gas mixtures. For some of the gases, the signal was attenuated by a factor of 3 to limit the occurrence of an ADC overflow to a few percent. The data were read out by a PC based data acquisition system.

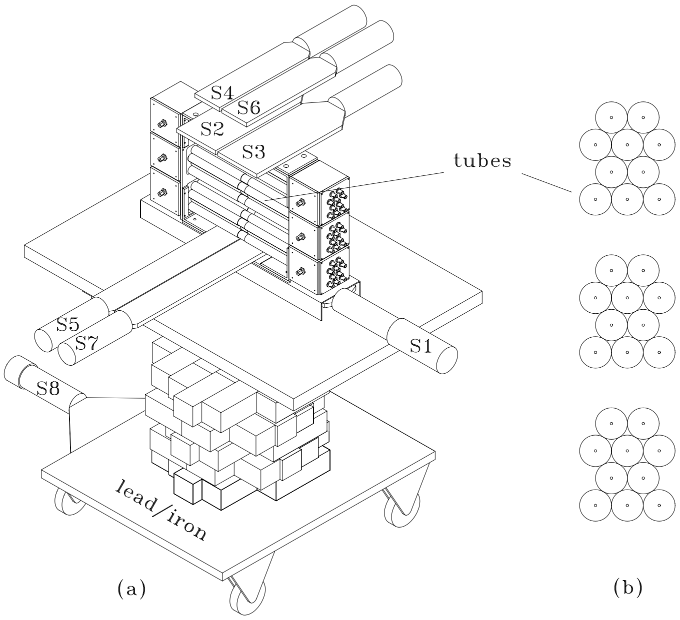

Fig. 1. Perspective (a) and end (b) views of the test chamber.

The pressure in the tubes was controlled by bubbling the output gas through $\sim$2 cm of water and the flow rate was such that the chamber gas volume was replaced about every five hours. Most of the data were collected using pre-mixed gases [8], where the minor content concentration was controlled to within $\pm$2%. For some data runs, we mixed our own gas. The relative mixture was adjusted to reproduce the pulse height measured with the pre-mixed gas to within a few percent. This should reproduce the relative fraction in the pre-mixed gas to within a few percent since the pulse height is very sensitive to the helium fraction.

3 Drift Velocity Determination

The data used in the spatial and dE/dx resolution measurements were required to have a pulse height (ADC) which is about five standard deviations above the pedestal peak. This cut is highly efficient except for a cosmic ray passing very close to the edge of a cell. The pedestal distributions were obtained in events with a hit pattern consistent with that produced by a cosmic ray. The hits associated with the hit pattern were excluded from the pedestal distributions.

The pedestal distribution for each wire was fitted to a bifurcated Gaussian to extract the peak and width.

The drift time to distance relationship was extracted using an iterative procedure. A rough estimate of the relationship was used as the seed. A track was projected into a tube excluded from the fit and the measured drift time was plotted as a function of the projected distance. The drift time distribution was then fitted for each bin of the projected distance to produce a new time to distance relationship. The distributions for each group of ten wires were combined to increase statistics. The procedure was repeated two or three times before the time to distance relationship converged.

The chamber alignment was performed using ArC_2H_6 (50:50). Here we took advantage of the well-understood properties (e.g. saturated drift velocity) of the gas. The time offset (T_0) of each wire was adjusted so that all the timing distributions started at around zero. The relative wire alignments were then adjusted so that all the residual distributions centered at zero to within $\sim$20 μm. Minor T_0 adjustments were made for each gas mixture and operating voltage since the discriminator threshold was fixed.

The drift velocities measured for the various gas mixtures are shown in Fig. 2. All the helium-based gases are slower than ArC_2H_6 (50:50) but fast enough so that the charge may be collected in less than 0.5 μs for the 1 cm drift distance. The collection time will be longer in a magnetic field. We believe that the collection time will be acceptable for most e^+e^- experiments. The helium-ethane mixture has a higher velocity than the helium-propane mixtures which are in turn comparable or higher than those of the helium-isobutane mixtures. The measurements are compared with the MAGBOLTZ predictions [9] which calculate the drift velocities using the Maxwell electron transportation theory based on the measured electron cross sections. The measurements are consistent with the calculations at low electric field, $\lesssim$2 kV/cm. The results are also consistent with the measurements by other experiments [2,3,10]. All the helium-based gases saturate at much higher electric field in comparison with ArC_2H_6 (50:50). Figure 3 shows the drift velocity as a function of distance from the wire (r) for several gases operated at 2000 V. In this study, only ArC_2H_6 (50:50) was operated in the saturated region.

4 Spatial Resolution

The spatial resolution as a function of distance from the wire for the middle group of drift tubes is measured by interpolation from the top and bottom

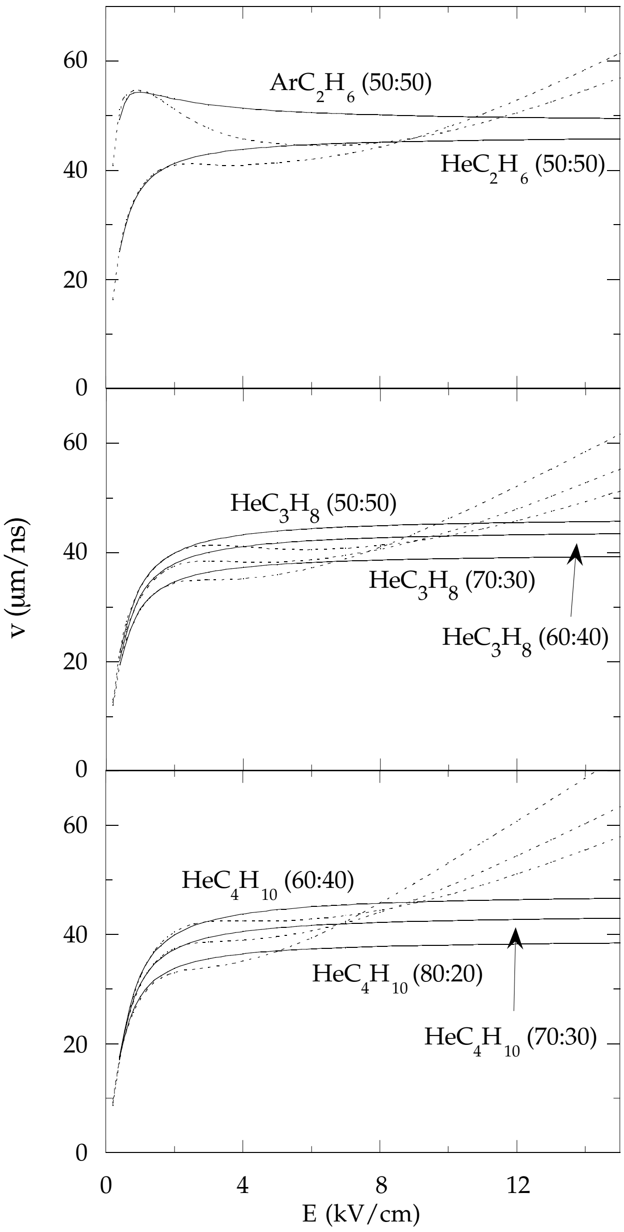

Fig. 2. Dependence of the drift velocity on the electric field. The MAGBOLTZ predictions are shown as dashed lines.

groups. The results are shown in Fig. 4. The resolution deteriorates near the wire because of primary ion statistics. The degradation at large radius is due to diffusion. All gases show a similar distance dependence except HeC_2H_6 (50:50) which has somewhat worse resolution near the wire due to smaller number of primary ions per unit length.

The measured spatial resolution includes both the interpolation error and the systematic error due to wire misalignment and T_0 uncertainty. To avoid the systematic problem, the resolution has been measured using a triplet of wires as shown in Fig. 5. The sum of the drift distances equals the outer radius of

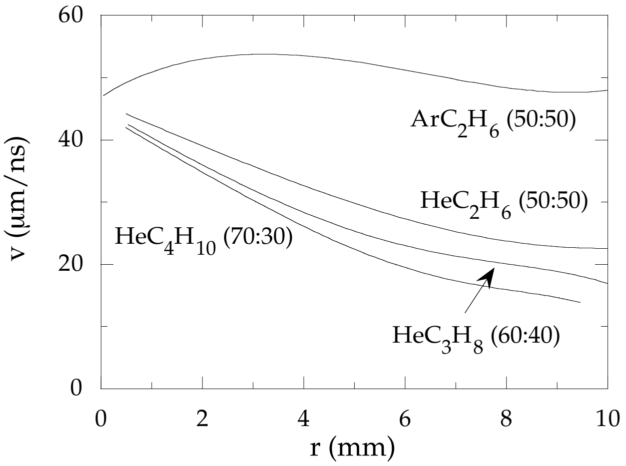

Fig. 3. Measurement of the drift velocity as a function of distance from wire (r) for various gas mixtures at 2000 V.

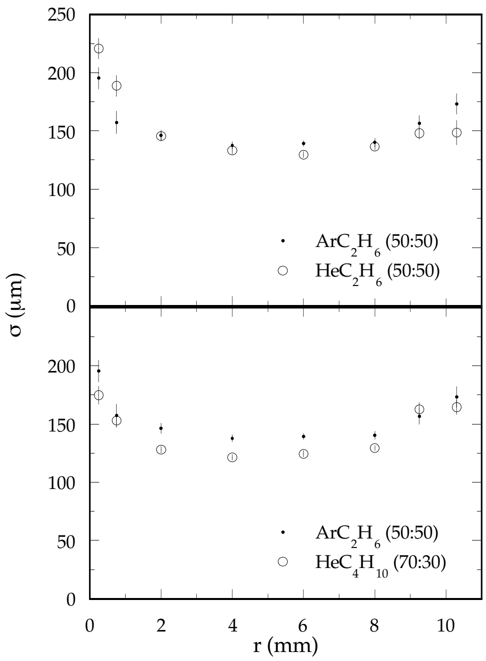

Fig. 4. The spatial resolution as a function of distance from wire (r) for ArC_2H_6 (50:50), HeC_2H_6 (50:50), and HeC_4H_{10} (70:30) at 2000 V.

the tubes:

$$\frac{1}{2}(d_1 + d_3) + d_2 = R_0. \tag{1}$$

The spatial resolution is $\sqrt{2/3}$ of the width of this drift distance sum distribution. In this technique, the relative misalignment and T_0 uncertainty cause a global shift of the distribution without affecting the width. In principle, the measured spatial resolution is the average across the whole tube. However, there is a slight bias against a track passing close to the edge of a tube because the pulse height may be too small to satisfy the minimum pulse height requirement to be considered as a hit to form a triplet.

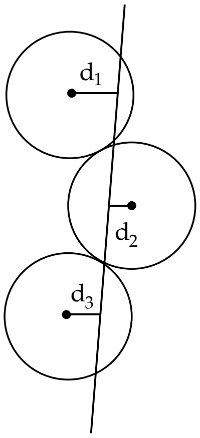

Fig. 5. A triplet of wires used to measure the spatial resolution.

The drift distance sum distributions of a triplet for ArC_2H_6 (50:50) and HeC_4H_{10} (70:30) are shown in Fig. 6. The distribution for HeC_4H_{10} (70:30) is narrower, corresponding to better spatial resolution. The resolution is extracted by fitting the distribution to a Gaussian over a polynomial background. The dependence of the spatial resolution on the discriminator threshold is shown in Fig. 7. The nominal value of 50 mV set through out the experiment is a reasonable compromise between good resolution and low noise. The spatial resolution of various gas mixtures is summarized in Fig. 8 for several operating voltages. The best resolution achieved for every helium-based gas is better than ArC_2H_6 (50:50). For the helium-isobutane mixtures, the 60:40 mix yields the best resolution, at 71.3 ± 0.5 μm. The result on HeC_2H_6 (50:50) is comparable with the measurement by Uno *et al.* [2] The resolution for HeC_4H_{10} (80:20) is significantly better than that of Playfer *et al.* [3] The optimal operating voltages for HeC_2H_6 (50:50), HeC_3H_8 (60:40), and HeC_4H_{10} (70:30) are similar to that of ArC_2H_6 (50:50). A mixture with more helium can operate at lower voltage and vice versa.

It is evident from Fig. 8 that the resolution of the helium-based mixtures improves as the hydrocarbon content is increased. This is due to the increase in the number of primary ions per cm (N) [11]. Figure 9 shows the best achieved resolution as a function of N. The dependence on N can be described by

$$\sigma(\mu m) \sim 440/\sqrt{N}. \tag{2}$$

This is consistent with the naive expectation based on ion statistics.

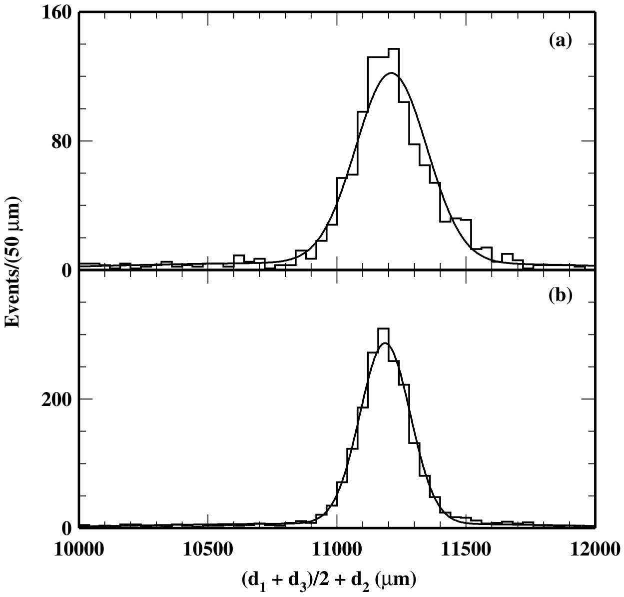

Fig. 6. The sum of the drift distances of a triplet for (a) ArC_2H_6 (50:50) and (b) HeC_4H_{10} (70:30). The curves show fits to the data as described in the text.

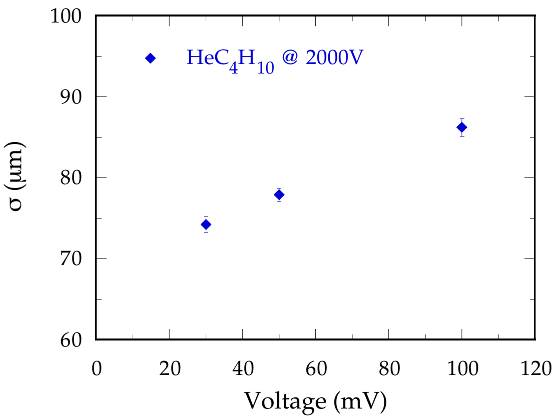

Fig. 7. The dependence of the spatial resolution on the discriminator threshold voltage.

5 Relative Gas Gain

The gas gains for the various gas mixtures are compared with ArC_2H_6 (50:50) by measuring the peak of the pulse height spectrum. The peak is determined by fitting the spectrum to a Landau distribution. The peak averaged over 30 wires for various voltages is shown in Fig. 10. The gain for HeC_2H_6 (50:50),

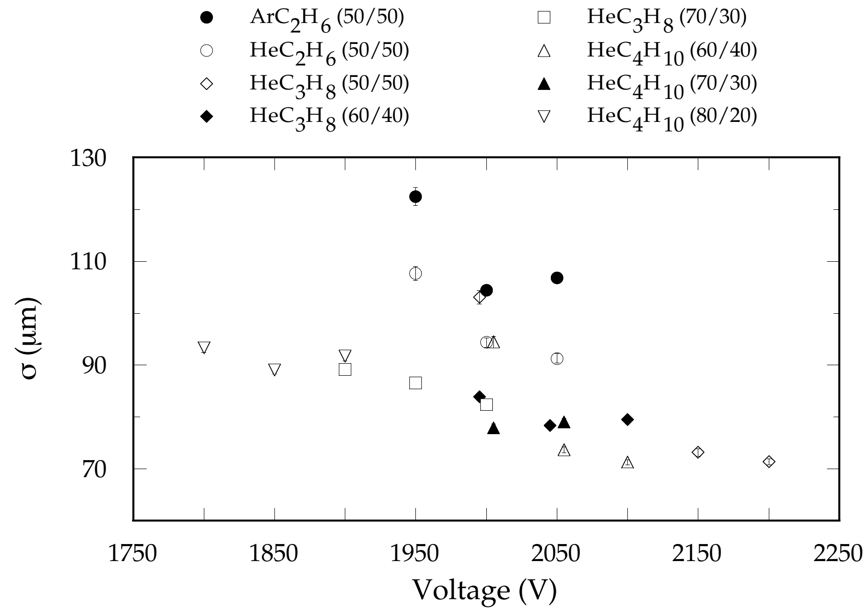

Fig. 8. The spatial resolutions of various gas mixtures as a function of the operating voltage.

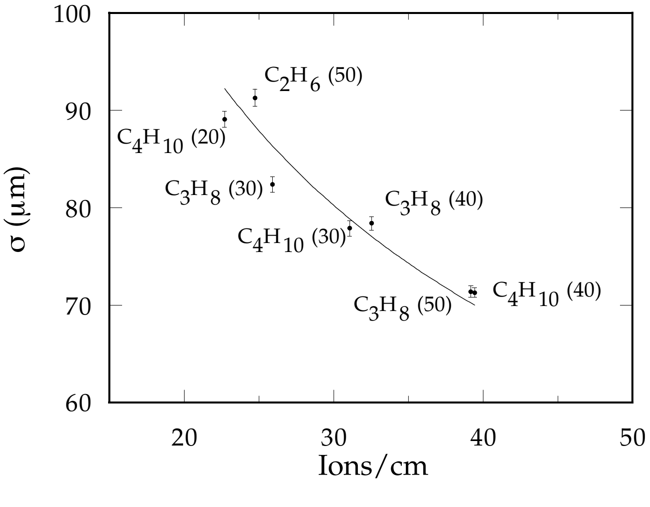

Fig. 9. The spatial resolutions of various helium-based gas mixtures as a function of the number of primary ions per cm. The percentage of hydrocarbon in a mixture is indicated by the number in the parenthesis. The curve shows a fit to the data of the form $1/\sqrt{N}$.

HeC_3H_8 (60:40), and HeC_4H_{10} (70:30) is similar to ArC_2H_6 (50:50), while HeC_3H_8 (50:50) and HeC_4H_{10} (60:40) have lower gain and HeC_4H_{10} (80:20) has higher gain. The mixtures with higher helium content have higher gain and can operate at lower voltage and achieve good spatial resolution.

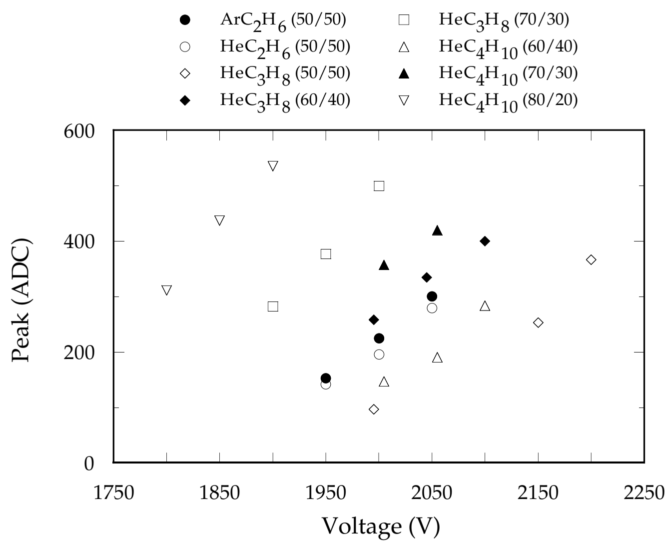

Fig. 10. The peak of the pulse height distribution for various gases at several operating voltages.

6 dE/dx Resolution

The dE/dx resolution depends on the number of hits used to calculate the average energy loss. The resolution is measured using 35 hits by combining several events. This simulates the average number of hits expected for a typical track in the CLEO III drift chamber. There are three corrections to the pulse height. The first is the correction for the variation in the pulse height due to different path lengths in a tube. The path length correction was calculated from the measured drift distance by assuming the track is perpendicular to the wire. The correction factor was limited to be less than 2.5 by requiring the hits to be within the inner 92% of the tube. The density variation due to pressure or temperature change was corrected about every two hours by adjusting the peak of the pulse height spectrum. The peak was extracted by fitting the pulse height spectrum combined from 30 wires to a Landau distribution. The relative gains between wires were measured by fitting the Landau spectrum of individual wires. The procedure was iterated until both the density and gain corrections converged.

The dE/dx resolution is measured using a truncation technique. Here only a fraction (e.g. 60%) of the hits are used in the energy loss calculation. The hits are ordered according to their pulse heights, from small to large, with the lowest f% (e.g. $f = 60$) of the hits used for the calculation. This procedure converts a Landau spectrum into a Gaussian-like spectrum. The resolution is then defined as the ratio of the width of the Gaussian to the pedestalsubtracted peak. The parameters are extracted by fitting the spectrum in the $^{+2\sigma}_{-3\sigma}$ region in order to reduce the sensitivity to the non-Gaussian tail. Figure 11 shows the mean pulse height from the lower 60% of the hits for HeC_3H_8 (60:40) at 2000 V. It is evident that the distribution is quite Gaussian. The resolution as a function of the truncation fraction for ArC_2H_6 (50:50) and HeC_3H_8 (60:40) is shown in Fig. 12. The resolution has a broad minimum at $\sim$ 60%. Other gases show a similar dependence. The measured resolution at various operating voltages is shown in Fig. 13. All the gases give similar resolution. We are not able to observe better resolution for some of the mixtures which have somewhat higher number of primary ions per unit length than ArC_2H_6 (50:50). This is probably due to the fact that there is still a considerable momentum (dE/dx) spread in the accepted tracks since the lead/iron filter only provides a low momentum cutoff.

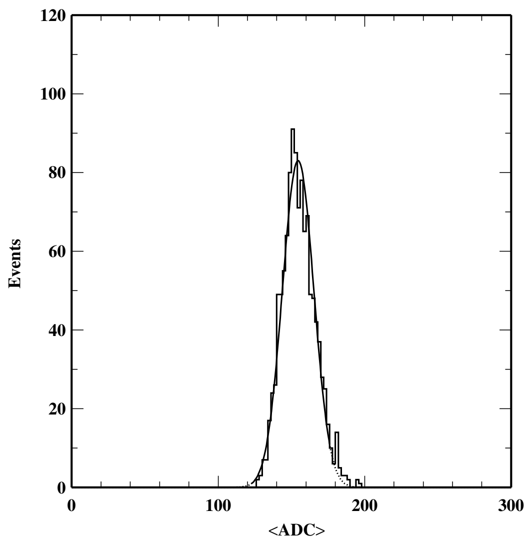

Fig. 11. The mean pulse height from the lower 60% of the hits for HeC_3H_8 (60:40) at 2000 V. The curve shows a Gaussian fit described in the text.

7 Conclusion

We have measured the properties of several helium-based gas mixtures as well as ArC_2H_6 (50:50) using cosmic rays. Our studies show that helium-based gases have better spatial resolution than ArC_2H_6 (50:50) under similar

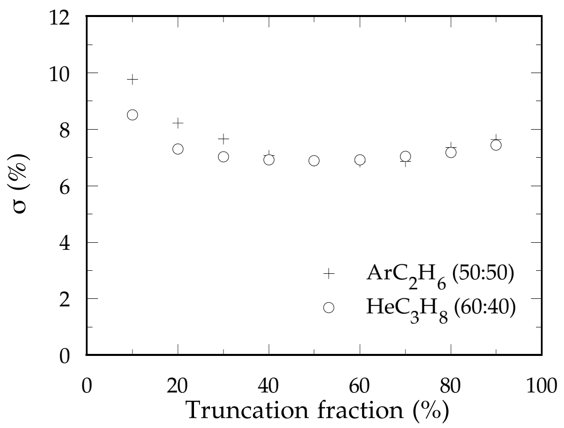

Fig. 12. The dependence of the dE/dx resolution on the truncation fraction for ArC_2H_6 (50:50) and HeC_3H_8 (60:40).

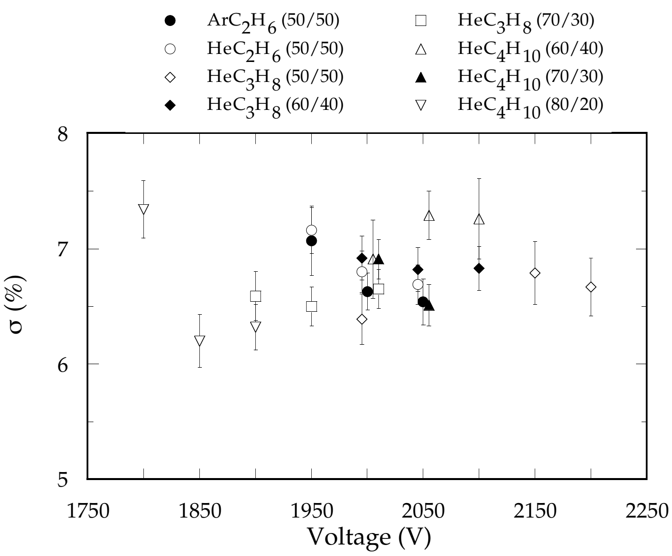

Fig. 13. The dE/dx resolution for the various gas mixtures at several operating voltages.

operating condition, while the dE/dx resolution is comparable. Helium-based gases are therefore good candidates for $\phi, \tau c$, and b factory drift chambers.

The determination of the appropriate fraction of hydrocarbon for a particular experiment depends on physics requirements. For example, in an experiment where multiple scattering is important, a low hydrocarbon content is desired. If multiple scattering is not an important concern, then increasing the hydrocarbon content will improve the spatial and dE/dx resolution of the detector due to the increase in the number of primary ions per cm. Thus the final selection of the gas will be dictated by whether the most important physics is dominated by low or high momentum tracks.

8 Acknowledgment

This work was supported in part by the U.S. Department of Energy. K.K.G thanks the OJI program of DOE for support. The authors wish to thank R. Galik and J.G. Smith for many helpful discussions.

References

[1] W. Zimmermann *et al.*, Nucl. Instr. and Meth. **A243**, 86 (1986).

[2] S. Uno *et al.*, Nucl. Instr. and Meth. **A330**, 55 (1993).

[3] S.M. Playfer *et al.*, Nucl. Instr. and Meth. **A315**, 494 (1992).

[4] V. Cindro *et al.*, Nucl. Instr. and Meth. **A309**, 411 (1991).

[5] P. Burchat *et al.*, Nucl. Instr. and Meth. **A316**, 217 (1992).

[6] "The CLEO III Detector, Design and Physics Goals", Cornell Laboratory of Nuclear Science Report CLNS 94/1277 (1994).

[7] D. G. Cassel *et al.*, Nucl. Instr. and Meth. **A252**, 325 (1986); Y. Kubota *et al.*, Nucl. Instr. and Meth. **A320**, 66 (1992).

[8] The gases were supplied by AGA, Gas Technics of Ohio, Liquid Carbonic, and Matheson.

[9] S.F. Biagi, Nucl. Instr. and Meth. **A283**, 716 (1989).

[10] J. Va'vra *et al.*, Nucl. Instr. and Meth. **A324**, 113 (1993).

[11] F.F. Rieke and W. Prepejchal, Phys. Rev. **A6**, 1507 (1972).